BUTTERWORTH HEINEMANN

Polymer Vol. 36 No. 12, pp. 2355–2362, 1995

0032-3861/95/$10.00 + 0.00

The relationship between slow crack propagation and tensile creep behaviour in polyethylene

P. A. O'Connell, M. J. Bonner, R. A. Duckett and I. M. Ward*
IRC in Polymer Science and Technology, University of Leeds, Leeds LS2 9JT, UK
(Received 7 February 1994; revised 28 September 1994)

The creep characteristics of drawn samples of a number of grades of polyethylene have been studied over a range of applied stresses and strains. In each case, the data allowed a unique and reproducible true stress:strain:strain rate surface to be determined. These data have been used in a new computer-based model for the mechanism of craze growth during the initiation of slow crack propagation. Using the model it has been possible to define the contribution the creep of the drawn material makes to craze growth and ultimately to the failure of the craze.

(Keywords: slow crack propagation; tensile creep behaviour; polyethylene)

INTRODUCTION

It is well known that the presence of a flaw or crack leads to a stress concentration at the crack tip, which, in order to prevent the formation of a stress singularity, produces a yield zone. Ahead of this yield zone, the bulk material is subjected to a complicated tri-axial stress state, the exact form of which depends on the applied bulk load and the size and shape of the crack. Within the yield zone itself are small voided regions and as the crack grows, these voided regions grow and join up to form an essentially fibrillar structure, which is generally described as a craze. These fibrils extend with time until eventually a failure criterion is satisfied and rupture occurs.

Work by Bhattacharya and Brown[1] has identified the processes involved in the growth of such a craze and these are shown schematically in *Figure 1*. At the craze tip material is continually yielding to form new voided material which in turn creates new fibrillar material. At the tip of the crack, the fibrils grow by the drawing in of new material at the bulk/fibril interace and the subsequent creep of this drawn material. It was also shown[1] that the craze increases in both length and thickness linearly with time until fibril failure occurs, followed by rapid crack growth and ultimate failure of the sample. The time for fibril failure to occur can be a significant proportion of the total failure time and it seems likely then that formation and deformation of the fibrils are a major factor in the lifetime of such materials. Recently, Cawood *et al.*[2] have shown a strong link between the creep response of a material and its stress crack performance. The work to be described in this paper concentrates on measuring the creep response of a range of materials and then linking these with experimental crack growth data to model more quantitatively the processes involved in craze growth up to crack initiation.

*To whom correspondence should be addressed

This work is part of a larger investigation into the mechanisms involved in both craze and crack growth in polyethylene and also the degree to which the material parameters affect these mechanisms.

For the purpose of this paper it is helpful to define the stresses which occur at or near the craze. These are shown schematically in *Figure 1*. Samples are loaded to an applied *bulk* stress of σ_B. Due to the stress concentration effect of the crack, there is a higher *effective* stress σ_E acting along the bulk/fibril interface. Finally, the *true* stress (σ_T) acting on any given section of the fibril is given by the product of the effective stress on the interface and the draw ratio of that section of the fibril and clearly varies along the length of the fibril.

EXPERIMENTAL

Materials

The current research has involved studies of a range of polyethylenes and data from two of these are presented here: an ethylene homopolymer (HP) and an ethylene copolymer (CP), for which the material characteristics are listed in *Table 1*. The morphology of each grade was varied by either quench cooling ($>80°C\,min^{-1}$) or controlled slow cooling at $2°C\,min^{-1}$. The materials were then characterized by their resulting density and yield stress. As can be seen from *Table 1* an increase in density, which is associated with an increase in crystallinity, leads to an increase in the conventional yield stress (measured at room temperature and a strain rate of $10^{-3}\,s^{-1}$).

Creep behaviour

Creep tests have been carried out in a separate investigation on both the isotropic and drawn material using purpose-built creep machines and some of the results will be used here. Details of the creep testing procedures may be found in reference 3. In brief,

dumb-bell samples (gauge length = 16 mm, width = 2 mm) of the material were cut from an isotropic sheet approximately 200 μm thick. These were loaded into a tensile testing machine and drawn at room temperature and an initial strain rate of $5 \times 10^{-3}\,s^{-1}$. The samples invariably yield and form a neck and it is the draw ratio of material having passed through the neck region which is defined as the natural draw ratio (λ_{nat}). As the extension proceeds, the neck moves through the isotropic material eventually reaching the shoulders of the dumb-bell. By further extension it is then possible to obtain drawn samples at draw ratios above λ_{nat}. These drawn samples were subsequently loaded into creep rigs and a range of initial stresses applied. By means of a displacement transducer attached to the lower end of the sample, the incremental strain and strain rate in the sample could be followed. The true stress, total strain and true strain rate in the sample were then determined by taking into account the initial draw ratio and followed throughout the course of a run. By using a range of initial conditions it was thus possible to build up a complete stress:strain:strain rate profile for the material.

Crack growth data

Crack growth data have been supplied by BP Chemicals (Grangemouth R&D Centre) using the single edge notch (SEN) testing geometry (*Figure 2*). The testing geometry remained constant for all tests, the only variable being the applied bulk stress. Using a sliding cathetometer, measurements were taken of the crack opening displacement (*COD*) as a function of time, where the *COD* is the length of the fibrils at the base of the craze (*Figure 1*). Because of the plane stress skin which occurs with these specimens, the measurements of the *COD* were taken from the centre of the specimen. Tests were carried out for the quenched HP at a bulk stress of 2 MPa ($K_I = 0.41\,MN\,m^{-3/2}$) and for quenched HP and slow cooled CP at bulk stresses of 3, 4 and 4.5 MPa ($K_I = 0.62$, 0.83 and $0.93\,MN\,m^{-3/2}$, respectively).

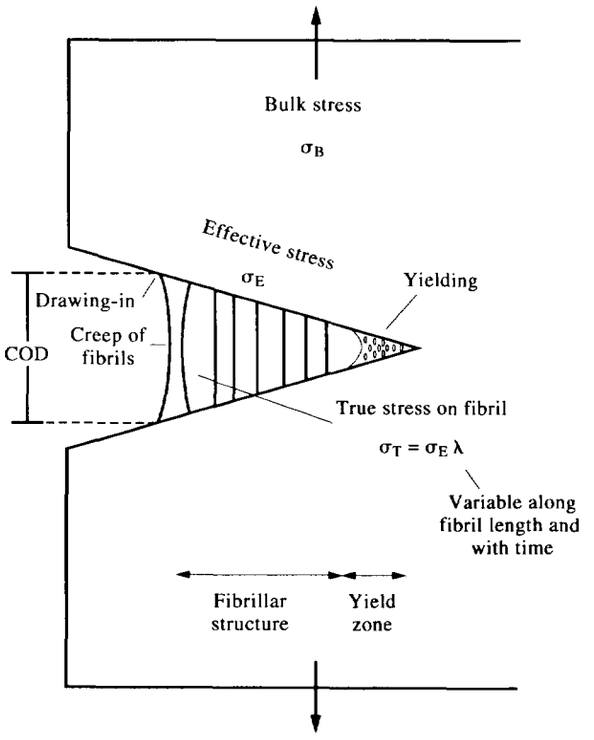

Figure 1 Schematic diagram showing the model for craze growth and the processes involved

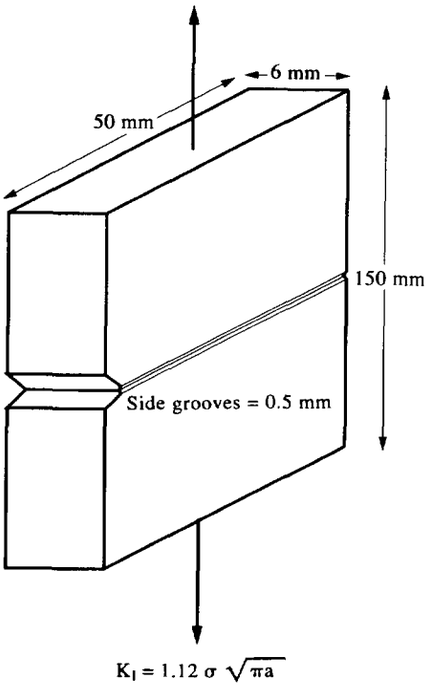

Figure 2 Single edged notched fracture specimen

Table 1 Material characteristics

Material	Cooling rate[a]	Branch content (per 1000 carbons)	M_w	M_n	Density ($kg\,m^{-3}$)	Yield stress (MPa)	Natural draw ratio	Limiting draw ratio
HP	S	<0.1	131 000	19 100	966	29.3		
HP	Q	<0.1	131 000	19 100	947	21.8	9.75	16
CP	S	1–2	156 000	17 000	955	25.2	8.7	13
CP	Q	1–2	156 000	17 000	943	19.7		

[a] Q, quenched at $>80\,°C\,min^{-1}$; S, slow cooled at $2\,°C\,min^{-1}$

RESULTS

Creep behaviour

Creep data for the drawn material are presented in the form of Sherby–Dorn plots[4], where the $\log_{10}$ strain rate is plotted against the strain (or draw ratio) as it evolves during a creep test at constant nominal stress. The data typically show two distinct regions (*Figure 3*), the first where the strain rate falls rapidly with strain and a second where the strain rate falls less rapidly with strain. The end point in the data is the point at which the sample ruptures.

It has been shown elsewhere[5] that the first region extends until the strain reaches the maximum value it had during the initial drawing process. The data in the second region were analysed as follows. As the strain in the sample is increased, the true stress was calculated assuming deformation at constant volume. The test could then be represented graphically by a series of points in stress:strain:strain rate space. By using a wide range of initial stresses it was found that the data points from each creep test described reproducible trajectories across a unique stress:strain:strain rate surface. It is useful to consider constant strain (draw ratio) sections across this surface. This is shown in the form of $\log_{10}$ strain rate *versus* true stress plots at constant draw ratio in *Figures 4* and *5* for the quenched HP and slow cooled CP materials, respectively. As mentioned above, the creep data show an abrupt end point where the samples fail. Over the range of stresses and strain rates examined, the strain at which this occurs appears to be constant for each of the materials studied. This limiting draw ratio then defines a failure criterion and the values for the natural and limiting draw ratios for the two materials are included in *Table 1*.

Given that the surface is unique, then for a sample subjected to any given initial stress and strain conditions (within the region of this surface) its subsequent route over the surface must also be unique, and moreover the time taken to cover the route will be uniquely defined. *Figures 4* and *5* show such routes over the surface for each of the two materials assuming the samples were both loaded to a nominal undrawn stress of 23 MPa. It is clear then that the time for the sample to reach the limiting draw ratio under any given initial conditions can be calculated, giving in effect a failure time under those conditions.

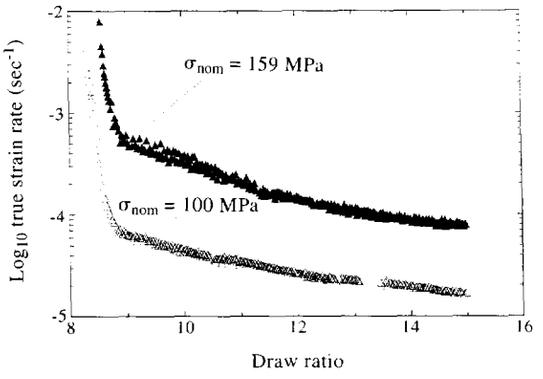

Figure 3 Sherby–Dorn plots for polyethylene homopolymer at different initial stress levels

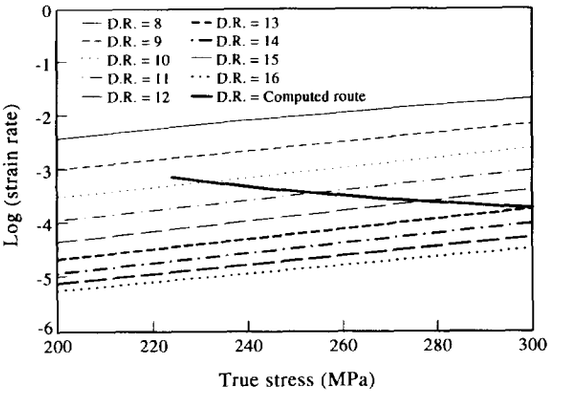

Figure 4 $\log_{10}$ (strain rate) *versus* true stress at constant draw ratio for polyethylene homopolymer. The draw ratios are indicated. —, Computed route

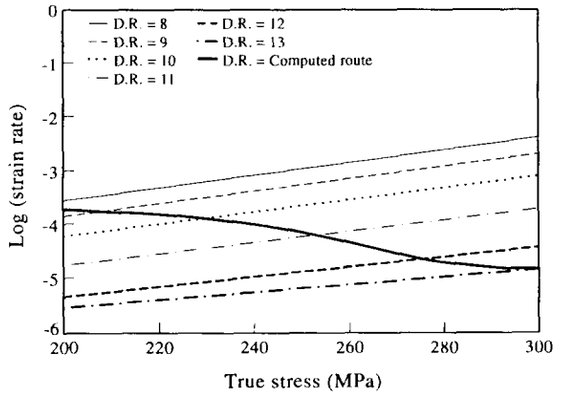

Figure 5 $\log_{10}$ (strain rate) *versus* true stress at constant draw ratio for polyethylene copolymer. The draw ratios are indicated. —, Computed route

Crack growth data

The crack growth data were supplied in the form of *COD versus* time curves for each of the applied bulk stresses. Typically these consisted of an initially linear portion followed by an accelerating rate (*Figure 6*). The gradient of the linear portion simply gives the *COD* rate. From experimental observation, the point at which the *COD* rate starts to accelerate is associated with the first signs of fibril failure at the base of the craze, with failure occurring in the mid-rib of the fibril, and thus gives a failure time, T_f. *Table 2* lists the *COD* rate and failure time for the two materials over the range of applied bulk stresses.

If the linear region is extrapolated to zero time, it is seen that the intercept is non-zero and positive. This is associated with an initial damage zone formed at the tip of the crack during the notching procedure, the size of which appears to be relatively independent of the applied bulk stress and with an average value of 63.6 μm for the HP:Q material shown in *Table 2*.

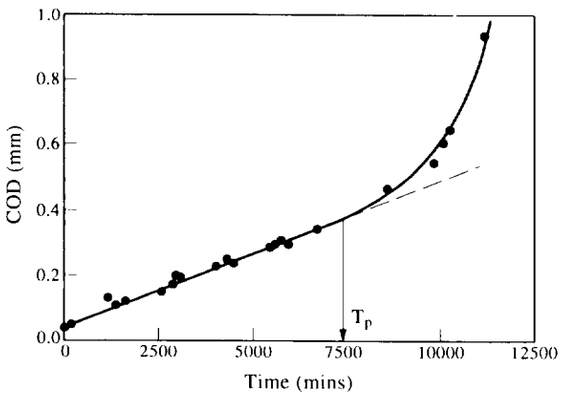

Figure 6 *COD versus* time for polyethylene copolymer at a bulk stress of 3 MPa

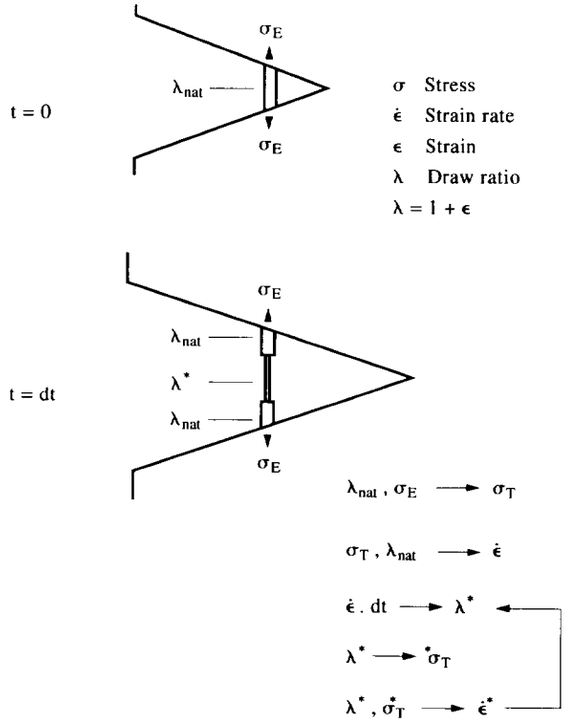

Figure 7 Schematic diagram of the model for fibril growth

MODEL FOR BEHAVIOUR

Computer routines have been written which attempt to model the formation and growth of a craze. The computer model is recursive, i.e. growth is calculated in successive time intervals Δt (typically ~20 s to 10 min, according to the strain rate at which the material creeps under the given initial conditions). At the moment the stress is applied ($t = 0$), an element of material at its natural draw ratio is assumed to bridge the interface (*Figure 7*). The length of this element is given by the initial damage zone length as discussed above (i.e. 63.6 μm as illustrated by the schematic model shown in *Figure 8*). Using the strain in this element and the effective stress (σ_E) assumed to be acting on the interface (a user defined variable), the true stress acting on this element (σ_T) can be found and the associated strain rate at this true stress and strain calculated from interpolation of the creep data. The element is allowed to creep at this rate for a time Δt, say 10 min, and the extension determined. During this time interval a new element of material is assumed to be drawn-in to its natural draw ratio from each interface at a rate which is fixed within the model. After 10 min the situation is as shown in *Figure 8*, where in this specific case the conversion rate has been set arbitrarily such that 2 μm of drawn material is created at each interface in each time interval (note that *Figure 8* shows the case for the initial element and one interface only, though this will clearly be mirror imaged on the second interface). The true stress and strain for each element can then be calculated and the respective strain rates interpolated from the creep data. Over the next time interval the

Element nos. / Time	Element 1	Element 2	Element 3	Element 4	Element 5
0 mins	63.6 μm	N/A	N/A	N/A	N/A
10 mins	63.6 μm + creep over 10 mins	2 μm	N/A	N/A	N/A
20 mins	63.6 μm + creep over 20 mins	2 μm + creep over 10 mins	2 μm	N/A	N/A
30 mins	63.6 μm + creep over 30 mins	2 μm + creep over 20 mins	2 μm + creep over 10 mins	2 μm	N/A
40 mins	63.6 μm + creep over 40 mins	2 μm + creep over 30 mins	2 μm + creep over 20 mins	2 μm + creep over 10 mins	2 μm

Figure 8 Schematic diagram of the computer model for fibril growth

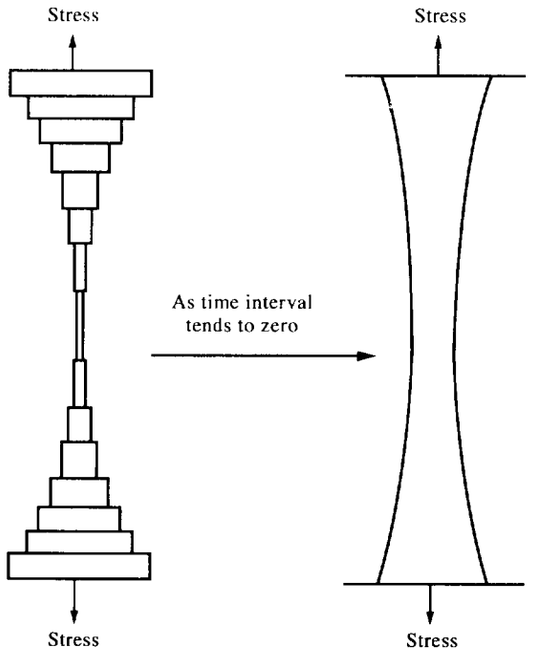

Figure 9 Schematic diagram of modelled fibril

extension in each element is calculated, the new strain and true stress determined for each, and with a new element being drawn-in. This whole process is then repeated, with each successive recursion both adding a new element and allowing the creep behaviour of all preceding elements to be determined (*Figure 8*) and the resulting total displacement calculated.

The modelled fibril thus ends up as a series of elements each of differing draw ratios and true stresses and thus creeping at a different rate; the draw ratio increases towards the centre or mid-rib of the fibril (*Figure 9*). The *COD* is simply the total fibril length, given by the addition of the lengths of all the individual elements.

It is possible then to simply calculate the *COD* rate at a given effective stress and assumed conversion rate by following the *COD* (fibril length) as a function of time and calculating the resulting gradient. The mid-rib element, which has been creeping for the greatest length of time will naturally have the largest draw ratio (*Figure 9*). If a critical draw ratio is assumed, beyond which the material fails, then the time for the mid-rib element to reach this limiting draw ratio at a given stress will determine the failure time of the fibril, T_f, at that stress.

Application to the experimental data

It should be pointed out at this stage that no assumptions are made on the magnitude of the effective stress, σ_E, acting on the bulk/fibril interface in a real craze and as yet there is no reliable method for measuring it. It is possible however to use the experimental crack growth data to infer the stress acting: as mentioned earlier, for a material at its natural draw ratio, the value of the applied stress will uniquely determine its subsequent route over the true stress:strain:strain rate surface and so uniquely determine the time to reach the critical draw ratio for that material, i.e. the failure time. Conversely, for a sample initially at its natural draw ratio, knowledge of the failure time must in turn uniquely determine the initial applied stress. As discussed above, the experimental failure time is known for each material at each of the applied bulk stresses from the upturn in the *COD*–time plot of the experimental SEN data (*Figure 6*). In order to use these data to determine the stress acting, the computer model was run using a range of effective stresses, and the strain (draw ratio) in the mid-rib element followed with time. At each effective stress the draw ratio increases with time, though the rate of increase falls with increasing strain (*Figure 10*). Eventually the strain in the mid-rib element reaches the limiting draw ratio and the fibril then fails. The time then for the mid-rib element to reach the limiting draw ratio defines the fibril failure time for that effective stress (*Figure 10*). By carrying this out over a range of effective stresses, the variation of the modelled fibril failure time with effective stress, σ_E could be determined (*Figure 11*). This then is a unique curve for each material, assuming the samples are initially at their natural draw ratio. By equating the experimental failure time from the SEN tests at a given bulk loading with this modelled failure time–stress relation it is possible to infer the effective stress that must be acting on the fibril via the bulk/fibril interface at that bulk loading. This is shown in *Figure 11*. The results for all bulk loadings on the quench cooled HP and slow cooled CP are given in *Table 2*. It should be emphasized that the effective stress inferred is dependent solely on

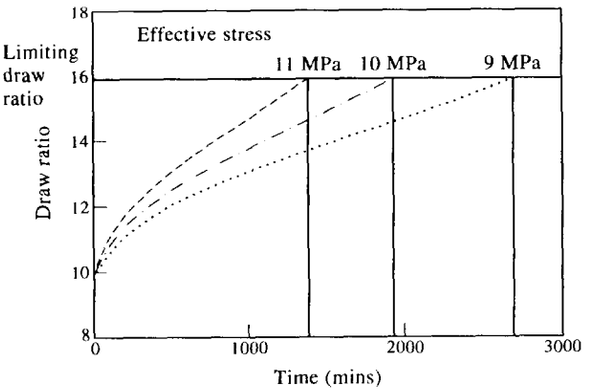

Figure 10 Mid-rib draw ratio *versus* time for polyethylene homopolymer

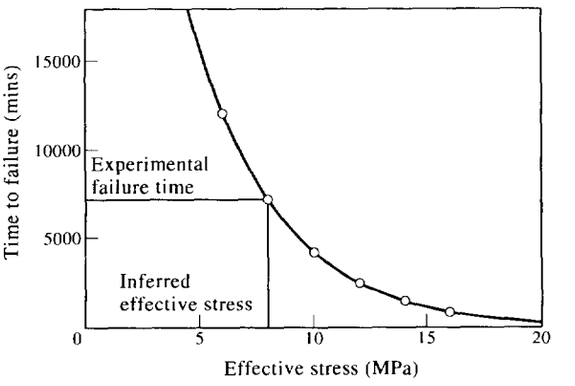

Figure 11 Modelled time to failure *versus* effective stress for polyethylene copolymer

Table 2 Experimental crack growth results and inferred effective stresses

Material	Bulk stress (MPa)	Failure time (min)	*COD* rate ($m s^{-1}$)	Inferred effective stress (MPa)	Initial *COD* size (μm)
HP:Q	2	10 500	2.78×10^{-10}	5.15	67.9
HP:Q	3	4 400	1.20×10^{-9}	7.30	68.7
CP:S	3	7 200	7.30×10^{-10}	7.98	
HP:Q	4	338	1.61×10^{-8}	15.47	55.6
CP:S	4	1 200	5.20×10^{-9}	14.83	
HP:Q	4.5	146	3.47×10^{-8}	18.38	62.2
CP:S	4.5	380	1.70×10^{-8}	19.26	

the creep and ultimate failure of the initial or mid-rib element, i.e. no assumption is made, nor needs to be made, about how this element was initially produced and its absolute size. It is also unnecessary to make assumptions about the behaviour of material away from the mid-rib (including both other elements within the fibril and the material which may be drawing-in at the interface).

The *COD* rate however is a function of the effective stress acting, the creep behaviour of all the elements of the fibril and the conversion rate of isotropic to drawn material occurring at the interface. The creep behaviour

has been experimentally determined, and the effective stress inferred above. To see the effect of conversion rate on *COD* rate, the computer model is run at the inferred effective stress for a given bulk loading using a range of conversion rates. At each conversion rate the total fibril length is calculated as a function of time to give a corresponding *COD* rate (*Figure 12* for quenched HP). It is clear from the graph that the *COD* rate is significantly greater than the corresponding conversion rate, indicating that the craze grows predominately by creep of the drawn material. However, this does not mean that the conversion of isotropic material at the interface can be ignored. The same initial damage zone size at all stresses coupled with a limiting draw ratio would imply that the maximum *COD* should be the same for all applied stresses if no conversion occurred at the interface. However, there is an approximately two-fold increase in the maximum *COD* over the range of stresses and this can only be accounted for by additional material being drawn-in at the higher stresses.

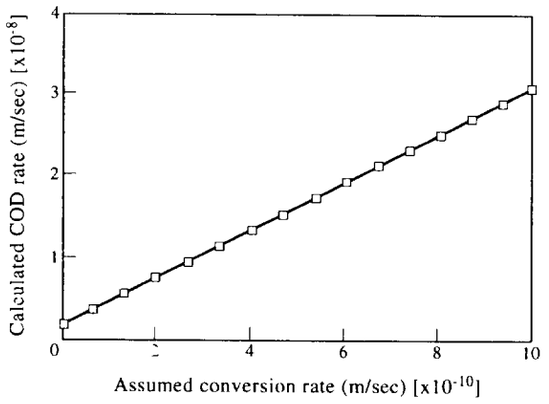

Figure 12 Calculated *COD* rate *versus* assumed conversion rate for polyethylene homopolymer at effective stress = 15.47 MPa

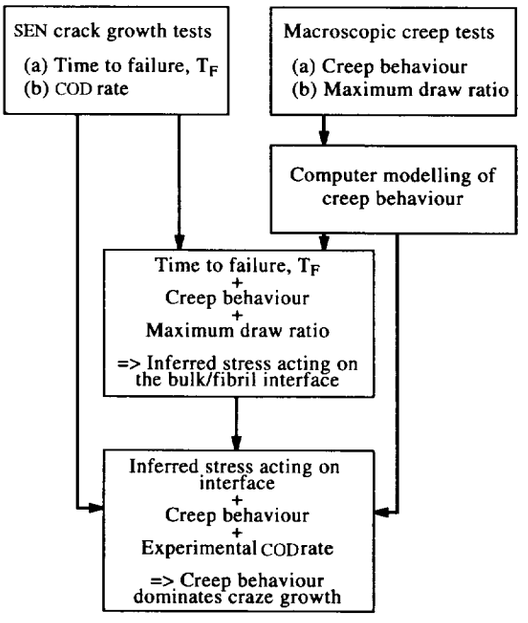

Figure 13 Flow diagram for data analysis

A summary of the way in which the experimental data have been integrated with the computer model to determine the effective stress and to define the contribution to craze growth from both creep and yielding is shown schematically in *Figure 13*.

DISCUSSION

The large amount of creep data collected has allowed an extensive region of the true stress:strain:strain rate surface to be mapped out in the drawn region. An accurate knowledge of this surface is then a powerful tool for predicting the behaviour of the drawn material under a wide range of conditions. For example the strain rate response for tests conducted at constant true stress or constant load may be deduced by the construction of the appropriate routes over the surface. This case is relevant to the present study, i.e. the surface is effectively being used to construct the strain rate:true stress response which would be obtained from a constant load creep experiment. In fact the situation is modelled as a constant effective stress on the interface, i.e. a constant stress on the isotropic material at the interface. Included in *Figures 4* and *5* are the computer generated routes over the surface for an effective stress on the isotropic material of 23 MPa (i.e. at the natural draw ratio of each material, the true stress is $\lambda_{nat} \times 23$ MPa).

It is clear from each plot that as the material increases in strain (and hence true stress), the strain rate is decreasing, i.e. the material is strain hardening. The degree to which the material strain hardens is obviously an important parameter in relation to craze growth, since a material with good strain hardening characteristics will rapidly reduce in strain rate and thereby extend the time to reach the failure criterion.

A useful measure of the degree of strain hardening is to take the gradient of the computer generated route over the surface, i.e. d[ln(strain rate)]/d(true stress) at constant force. For the two cases presented, the gradients are:

$$\text{HP:Q} \quad d[\ln(\dot{\varepsilon})]/d\sigma = -0.0073\ \text{MPa}^{-1} \qquad (1)$$

$$\text{CP:S} \quad d[\ln(\dot{\varepsilon})]/d\sigma = -0.0127\ \text{MPa}^{-1} \qquad (2)$$

The steeper gradient for the CP:S material is reflected in the increased failure time from the SEN tests over the HP:Q material (*Table 2*). This is similar to the idea proposed by Cawood *et al.*[2], who showed a very strong correlation between the gradient of the second region of the Sherby–Dorn plot (d[ln(strain rate)]/d(strain)) and the bottle stress crack performance (note that the true stress and strain are directly proportional). Care should be taken in this approach since the degree of strain hardening gives no information on either the natural draw ratio or the limiting draw ratio. However, the excellent correlation shown in reference 2 may indicate that both the natural and limiting draw ratios are intimately linked to the true stress:strain:strain rate surface (and hence strain hardening characteristics) and of course ultimately to the material morphology.

By concentrating on the failure criterion for the fibrils, it was necessary to look only at the central or mid-rib element in the computer model, i.e. the behaviours of the other fibril elements and of the material at the bulk/fibril interface have no effect on the failure criterion. Comparisons of the experimental failure times and those

predicted from the model using a range of stresses have shown that the effective stress, σ_E, acting on the interface varies from 5 to 18 MPa for applied bulk stresses of 2–4.5 MPa (*Figure 14*). It is commonly assumed that the interface stress is approximately the yield stress of the material, which is known to be very rate dependent. An example of this behaviour for the HP:Q material is shown in *Figure 15*. The range in effective stresses found here can be considered to be a reflection of this rate dependence. Equivalently, the creep rate of the drawn material is very dependent on the applied stress, and thus there is some 70-fold decrease in failure time for a relatively modest three- to four-fold increase in the effective stress acting.

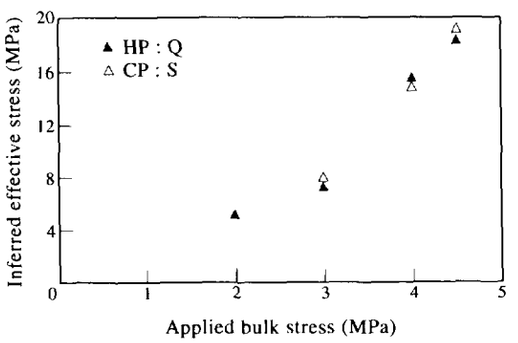

Figure 14 Variation of inferred effective stress with applied bulk stress: (▲) HP:Q; (△) CP:S

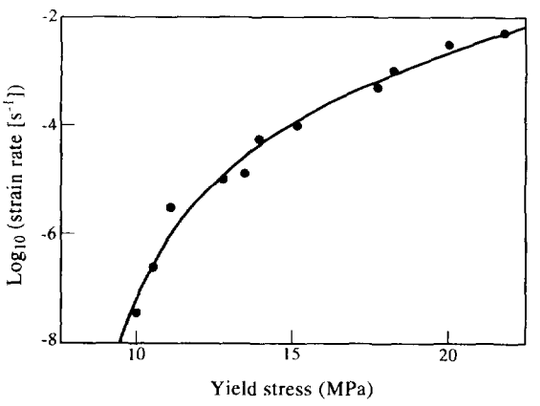

Figure 15 Log_{10} (strain rate) *versus* yield stress for polyethylene homopolymer

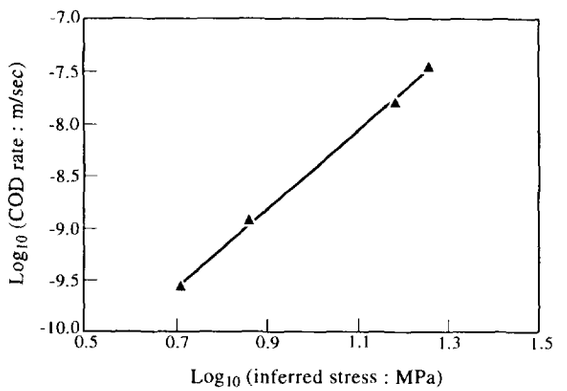

Figure 16 Log_{10} (experimental *COD* rate) *versus* log_{10} (inferred effective stress)

Finally, work by Chan and Williams[6] on the crack velocity in an almost identical grade of polyethylene gave a relationship of the form:

$$V = A\sigma^4 \tag{3}$$

where A is a constant that depends on temperature and geometry. Using the same grade of polyethylene, Brown and Bhattacharya[7] found a similar equation for the velocity of the craze in the linear region of craze growth:

$$V' = A'\sigma^{4.2} \tag{4}$$

Previous work[8] has shown that the craze angle remains approximately constant during craze growth so that the growth of the craze in the crack direction is simply linearly related to the *COD*. In turn, this means that the *COD* rate is linearly related to the craze velocity. A $\log_{10}$–$\log_{10}$ plot of the experimental *COD* rates and the inferred stresses found in this study (*Figure 16*) shows excellent linearity, from which it is found that:

$$COD \text{ rate} = 4.14 \times 10^{-8}\sigma^{3.7} (\text{m s}^{-1}) \tag{5}$$

As can be seen, the exponent found in this study compares favourably with those found in the previous studies.

CONCLUSIONS

By manipulation of a comprehensive range of creep data, unique true stress:strain:strain rate surfaces have been constructed for two grades of polyethylene in the drawn state. The creep work has also shown that in the region of the surface studied the materials exhibit limiting draw ratios, beyond which the material will break.

Single edge notch crack growth experiments have shown that rapid crack propagation is preceded by the failure of the mid-rib of the fibrils at the base of the craze, indicating that it is the creep and failure of the mid-rib section which ultimately controls the failure lifetime. By construction of the appropriate constant load route over the surfaces, the relative strain hardening characteristics of each polyethylene grade have been deduced and this has given insight into the resulting stress crack performance.

A simple computer model has been derived for the yield and creep to failure of the fibrils at the tip of a crack in a polyethylene craze. This has shown that the *COD* rate and hence failure time is dominated by the creep to failure of the fibrils.

In considering only the failure criterion for the fibrils, it is necessary only to consider the behaviour of the central or mid-rib element of the fibril. Modelling this behaviour using the true stress:strain:strain rate surfaces for a range of grades of polyethylene should then allow a relatively quick method for ranking the materials in terms of possible stress crack resistance.

ACKNOWLEDGEMENTS

This work was carried out under a contract with BP Chemicals Ltd. We also wish to thank our colleagues at the BP Chemicals Grangemouth R&D Centre, especially Dr G. Capaccio, Mr A. D. Channell, Mr L. Rose and Dr E. Q. Clutton for their helpful advice and assistance and again Mr A. D. Channell for the experimental crack growth data.

REFERENCES

1 Bhattacharya, S. K. and Brown, N. *J. Mater. Sci.* 1984, **19**, 2519
2 Cawood, M. J., Channell, A. D. and Capaccio, G. *Polymer* 1993, **34**, 423
3 Wilding, M. A. and Ward, I. M. *Polymer* 1978, **19**, 969
4 Sherby, O. D. and Dorn, T. E. *J. Mech. Phys. Solids* 1956, **19**, 165
5 Bonner, M. J. unpublished work
6 Chan, M. K. V. and Williams, J. G. *Polymer* 1983, **24**, 234
7 Brown, N. and Bhattacharya, S. K. *J. Mater. Sci.* 1985, **20**, 4553
8 Huang, Y. and Brown, N. *J. Polym. Sci., Polym. Phys. Edn* 1990, **28**, 2007